AUTOMATED PREDICTION OF CRATER DEGRADATION DEGREE

Pedro Pina

CERENA
Instituto Superior Técnico
Universidade de Lisboa, Portugal

*Jorge S. Marques**

Institute for Systems and Robotics
Instituto Superior Técnico
Universidade de Lisboa, Portugal

ABSTRACT

A learning system that is able to predict the degradation state of impact craters on optical images is presented in this paper. It is based on the extraction of visual features along the crater rim together with the decision with a SVM classifier. The algorithm achieved a sensitivity of 89% and a specificity of 96% (preserved vs non-preserved) in a dataset of annotated craters from Mars.

***Index Terms*—** Impact craters, degradation measure, optical images, learning system.

1. INTRODUCTION

Impact craters are the most common structure on planetary surfaces. They have been highly studied and their number and density allow estimating the age of a surface. This led to the creation of complete catalogues up to a given dimension with the location of each individual crater. Initially, these catalogues were built from manual identification (e.g., Barlow and Robbins catalogues on Mars), but more recently there has been an effort to incorporate the results from automated detection algorithms and many contributions have been proposed [1, 2, 3, 4, 5].

Although craters density provides useful information about the age of planetary surfaces, their deformation gives important additional cues about the degree of erosion experienced within specific geological units (see examples in Fig. 1) and also how those degradation rates changed with time [6]. Unfortunately, there are no methods addressing this issue directly on optical imagery, nor objective criteria for a quantitative characterization of a crater degradation stage. This paper, intends to propose a first solution to characterize the preservation stage of craters based on the visual analysis of the crater rim using pattern recognition.

Section 2 discusses the problem and provides a visual preservation criterion based on the opinion of experts. Section 3 describes an algorithm to delineate the crater rim from optical images. Section 4 addresses the extraction of visual features along the rim and the learning algorithm used to predict the expert evaluations. Sections 5 and 6 describe the experimental setup used to evaluate the proposed method and presents the experimental results.

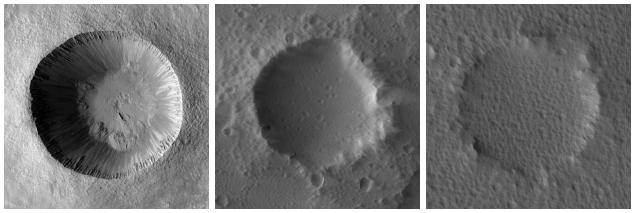

Fig. 1. Examples of Martian craters with different degrees of degradation [image credits: NASA/JPL/University of Arizona].

2. PROBLEM STATEMENT

The quantification of the state of preservation of impact craters is an important topic of research. Several efforts have been developed using topographic information extracted from digital elevation models (DEM) [7, 8]. These works sample the crater along radial directions and characterize the shape of the elevation profiles, *e.g.* trying to estimate the steepness of the walls, the degree of completeness of the rim, or the amount of infilling of the crater with sediments.

These approaches require the use of a DEM with very high resolution which unfortunately only exist for limited regions of planetary bodies. Therefore, this suggests the use of optical images which are much more wide spread with higher spatial resolution. For instance, the Context Camera (CTX) currently operating on Mars Reconnaissance Orbiter (MRO) provides a near complete coverage ($> 90\%$) of the red planet with images at 6 m/pixel resolution, while the global elevation coverage provided by the Mars Orbiter Laser Altimeter (MOLA) is 100s of meters. One of the few attempts in this direction is the work of Ambrose [9] for the Moon, which proposes 7 qualitative criteria (rays of eject, rim, fractured floor, flooded interior, major post-impacts, ejecta from other craters, and albedo) to build a quantitative degradation index.

*Partially funded by FCT [UID/EEA/50009/2013 and PTDC/EEI-PRO/0426/2014].

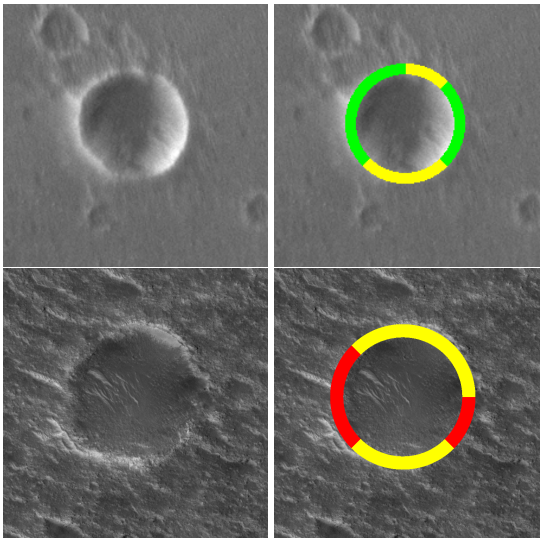

Fig. 2. Degradation code assignment performed by expert: preserved (green), degraded (yellow) and highly degraded (red) [image credits: NASA/JPL/University of Arizona].

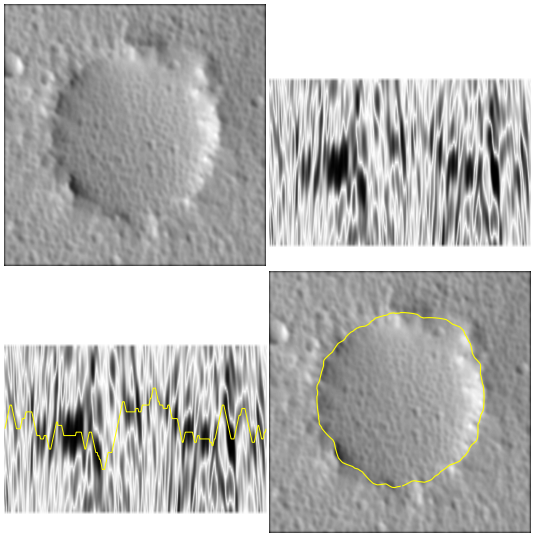

Fig. 3. Crater delineation: original image (up-left), edge map in polar coordinates (up-right), optimal contour in polar coordinates (bottom-left) and final contour (bottom-right).

The analysis of each of these criteria must be performed by a specialist and has to be repeated for each new crater.

In order to use a degradation index in large scales we need to develop an automated procedure. In this paper, we define a degradation criterion to be applied by an expert and propose an algorithm that learns to predict the value of the criterion in an automated way, solely based on the analysis of the crater rim.

Given the image of a crater with known center and radius, we divide the rim into 8 sectors with equal amplitude and assign a ternary label (number or color) to each sector, depending on its degradation status:

0. (green) preserved rim: pristine rim with sharp and non deformed edges;
1. (yellow) degraded rim: smoothed edges or moderate amount of deformation;
2. (red) highly degraded: very smoothed or absent rim.

Fig. 2 shows two examples and the respective color codes for each of the 8 sectors of analysis, assigned by an expert. The first crater is well preserved and the sectors are of types 0 and 1, while the second crater is more degraded and the sectors receive labels of types 1 and 2. Of course this labeling operation performed by an expert involves some subjectivity.

We now wish to automate this procedure by using a learning algorithm, able to extract information about each crater sector and classify each sector in one of the three labels. The approach proposed in this paper is based on the delineation of the crater rim, followed by the analysis of its contour. This will be addressed in the next two sections.

3. CRATER DELINEATION

The delineation of the crater rim poses several challenging difficulties since the edge information is usually very noisy and incomplete. Therefore, we use a dedicated algorithm recently developed by ourselves [10] to make this delineation, which combines intensity information extracted from the image with the geometric constraints imposed via Dynamic Programming.

The algorithm involves the following steps (see Fig. 3). First, the image of the crater is converted to polar coordinates, assuming that the crater center is known a-priori (which is the common situation). Then, an edge map is computed in polar coordinates using the vertical derivative (along the crater radial directions). The edge map is obtained using the logistic function

$$e(r,\theta) = \frac{2}{1+e^{sg(r,\theta)}} \ ,$$

which maps the vertical gradient intensity $g \in [0,+\infty[$ into an edge confidence $e \in [0,1[$.

Then, the crater contour is extracted by the minimization of an energy function using Dynamic Programming in polar coordinates. Please note that a perfect circle would correspond to a constant path in polar coordinates. The final step involves the conversion of the contour to Cartesian coordinates.

The algorithm is robust and performs well even in the case on very degraded craters. For additional details and validation please consult [10].

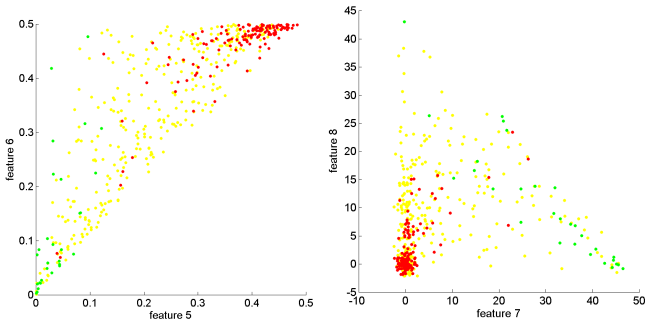

Fig. 4. Scatter plots of features 5, 6, 7, 8 for each of the three degradation types.

4. FEATURE EXTRACTION

The edge map contains important information about the crater (see Fig 3). A preserved crater should have sharp edges which correspond to deep valleys in the edge map. The extracted contour (in polar coordinates) should travel along the deep valleys and avoid high intensity regions.

The intensity profile of the edge map along the contour, $p(\theta)$, is therefore a rich source of information. We divide the edge map into 8 sections (vertical strips) and for each section we characterize the intensity profile using 6 percentiles, associated to percentages $p = 20k\%, k = 0, \ldots, 5$ and using an histogram with 11 bins

$$h(k) = \sum_{\theta \in \text{Strip}} b_k(p(\theta)) \qquad k = 0, \ldots, 10$$

where $b_k(p)$ denotes the characteristic function of bin k.

The shape of the contour is also taken into account. The delineated contour is estimated assuming that θ and r are multiple of $\Delta\theta = 1°$, and Δr. Furthermore, it is assumed that the transition between consecutive values of $r(\theta)$ can take three possible values: $0, \pm\Delta r$. We characterize all pairs of consecutive transitions and compute a co-occurrence matrix of all pairs of transitions (9 hypothesis). This leads to a feature vector with 9 features.

We have also measured the differences between the contour and an arc of circle in each sector, to obtain local geometric deformations. To be more specific, we compared the contour in polar coordinates with a constant in each sector and measured the area above the constant.

These four sets of features described above lead to a feature vector of 27 features associated to each crater sector. Fig. 4 displays the scatter plots of some of these features showing that there is a clear distinction between preserved (green) and highly degraded (red) craters. The degraded ones (yellow) lie in the middle.

		Predicted		
		0	1	2
Annotated	0	28	1	0
	1	48	215	54
	2	0	34	100

Table 1. Confusion matrix of the ternary decision system.

5. EXPERIMENTAL SETUP

The system was evaluated using a database of 60 Martian craters extracted from image ESP-011491-2090 acquired by the High Resolution Imaging Science Experiment (HiRISE). Each crater was divided into 8 sectors and each sector was labeled by an expert into one of the three degradation classes.

The algorithm was tested using a leave one crater out approach. This means that we have used the data from one crater (8 sectors) for testing and all the others for training the classifiers. This procedure is repeated until all craters are used for testing. In the training phase, we have first selected a subset of N_f features using the correlation index between each feature and the decision. Then, we trained two classifiers. The first classifier discriminates preserved from non-preserved sectors (class 0 vs the other two). The second classifier was trained to discriminate between degraded and very degraded sectors. Both classifiers were implemented using a Support Vector Machine (SVM) with Gaussian kernel. The output of these tests were evaluated using standard statistical criteria: sensitivity and specificity.

6. RESULTS

Fig. 5 shows the output of the proposed method and that of the expert labeling, assumed as ground truth. There is a good general agreement. Concerning the statistical evaluation, the proposed algorithm achieved a sensitivity of 89% and a specificity of 96% in the first decision (preserved vs non-preserved sectors) and a sensitivity of 75% and a specificity of 80% in the second decision (degraded vs very degraded). It is concluded that the second decision is more difficult than the first one. Table 1 shows the confusion matrix of the ternary classification system. There was no confusion between preserved and highly preserved sectors. Only the middle class is sometimes confused with one of the others.

7. CONCLUSIONS

This paper presents a first attempt to quantify the degradation state of craters from optical images. We propose a system that extracts information from the crater rim and produces an automated decision concerning the degree of preservation of each sector. The results are encouraging and suggest further improvements.

The next steps may include the testing of other image features and an improvement of the database by including additional examples and more annotators, in order to assess the performance of human annotators in this task.

It is also in our plans to confront this approach with those that use elevation information that permits a more reliable decision although constrained by the less amount of high resolution DEM data available.

8. REFERENCES

[1] E. R. Urbach and T. F. Stepinski, "Automatic detection of sub-km craters in high resolution planetary images," *Planet. Space Sci.*, vol. 57, pp. 880–887, 2009.

[2] R. Martins, P. Pina, J. S. Marques, and M. Silveira, "Crater detection by a boosting approach," *IEEE Geosci. Remote Sens. Lett.*, vol. 6, no. 1, pp. 127–131, 2009.

[3] S. Vijayan, K. Vani, and S. Sanjeevi, "Crater detection, classification and contextual information extraction in lunar images using a novel algorithm," *Icarus*, vol. 226, pp. 798–815, 2013.

[4] S. Jin, and T. Zhang, "Automatic detection of impact craters on Mars using a modified adaboosting method," *Planet. Space Sci.*, vol. 99, pp. 112-117, 2014.

[5] G. Salamunićcar, S. Lončarić, P. Pina, L. Bandeira, and J. Saraiva, "Integrated method for crater detection from topography and optical images and the new PH9224GT catalogue of Phobos impact craters," *Adv. Space Res.*, vol. 53, pp. 1798–1809, 2014.

[6] N. G. Barlow, "Constraining geologic properties and processes through the use of impact craters," *Geomorphology*, vol 240, pp-18–33, 2015.

[7] R. A. Craddock and T. A. Maxwell, "Crater morphometry and modification in the Sinus Sabaeus and Margaritifer Sinus regions of Mars," *J. Geophys. Res.: Planets*, vol. 102, no. E6, pp. 13,321-13,340, 1997.

[8] W. A. Watters, L. M. Geiger, M. Fendrock, and R. Gibson, "Morphometry of small recent impact craters on Mars: Size and terrain dependence, short-term modification," *J. Geophys. Res.: Planets*, vol. 120, pp. 226-254, 2015.

[9] W. A. Ambrose, "First-order relationships between lunar crater morphology, degree of degradation, and relative age: the crater degradation index", American Association of Petroleum Geologists Annual Convention, v. 15, p. 4, 2006.

[10] J. S. Marques and P. Pina, "Crater delineation by dynamic programming," *IEEE Geosci. Remote Sens. Lett.*, vol. 12, no. 7, pp. 1581–1585, 2015.

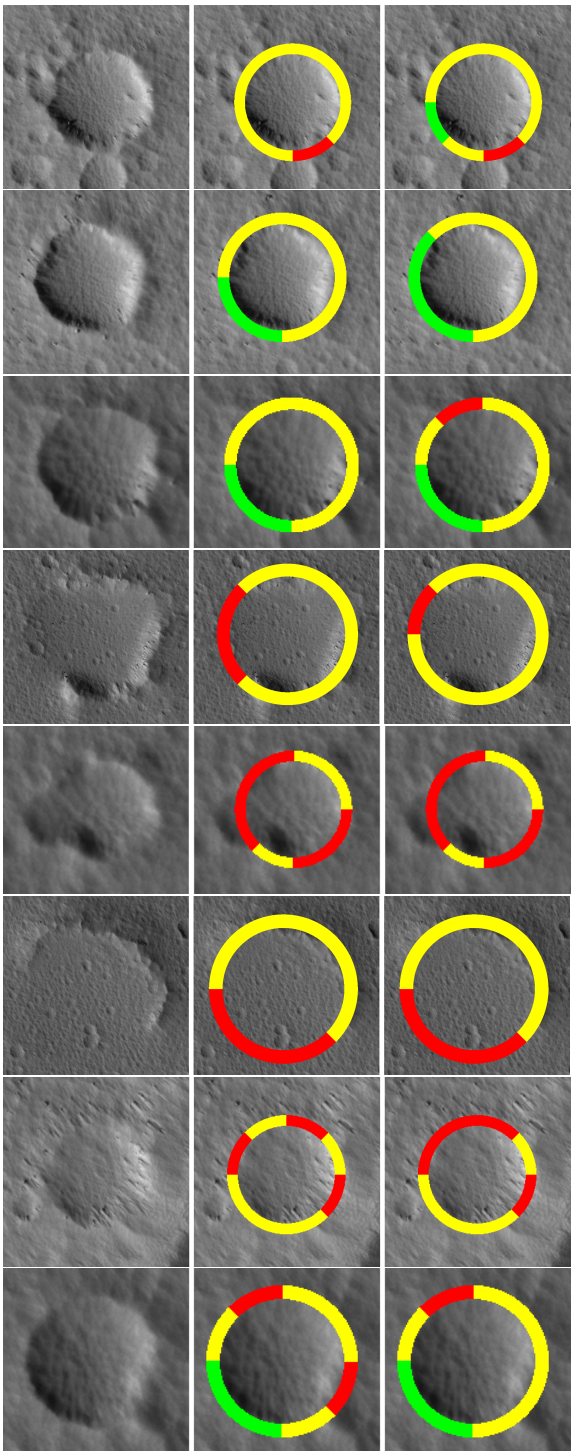

Fig. 5. Examples: original image (left); manual (center) and automated (right) label [image credits: NASA/JPL/University of Arizona].